Enhanced magnetic ordering in the heavy lanthanide Er metal under megabar pressures

Hongyu Liu,[1,2] Jing Song,[1,*] Wei Wu,[1] Baosen Min,[1,2] Sijia Zhang,[1] Shaomin Feng,[1] Xiancheng Wang,[1] and Changqing Jin[1,2,†]

[1]*Institute of Physics, Chinese Academy of Sciences, Beijing 100190, China*

[2]*School of Physical Sciences, University of Chinese Academy of Sciences, Beijing 100190, China*

(Received 19 November 2024; revised 10 February 2025; accepted 26 February 2025; published 7 March 2025)

Four-point electrical resistivity measurements were carried out on erbium (Er) metal and dilute magnetic alloy containing 0.5 at.% Er in superconducting Y for temperatures 3.5–295 K under pressures to 183 GPa in a diamond anvil cell. The magnetic ordering temperature T_o of Er appears to rise rapidly above 80 GPa. Y(Er) alloys display giant superconducting pair breaking ΔT_c per atomic percent as large as 19 K/at.% Er. The present results give evidence that, for pressures above 80 GPa, the exchange coupling J between Er ions and conduction electrons becomes negative, thus activating Kondo physics in this highly correlated electron system. We suggest that these anomalously high magnetic ordering temperatures are an unrecognized feature of the Kondo lattice state, providing another perspective for designing magnetic materials with high ordering temperature.

DOI: 10.1103/PhysRevB.111.125117

I. INTRODUCTION

Lanthanide elements are of particular interest from a fundamental perspective. Their partially filled $4f$ orbital leads to their complex crystal and electronic structures, hence yielding rich phase diagrams and unique properties. Tuning elemental lanthanide metals by pressure can reveal the intrinsic nature of a $4f$ electron without introducing chemical disorder. When compressed under extreme pressures, lanthanide systems could possibly enter a regime with magnetic instabilities, exhibiting many fascinating phenomena, such as Kondo lattice behavior [1], anomalous magnetism [2,3], unconventional superconductivity [4,5], and quantum criticality [6].

In lanthanide systems near a magnetic instability, the Doniach phase diagram [7–9] describes the competition between the Ruderman-Kittel-Kasuya-Yosida (RKKY) interaction and Kondo spin screening, governed by the negative exchange coupling J between magnetic ions and conduction electrons, as illustrated in Fig. 1. In such a Kondo lattice system, the magnetic ordering temperature (T_o) is predicted to increase initially with the magnitude of $|J|$, reach a maximum, and then decrease toward 0 K, marking a quantum critical point. Extensive attention has been devoted to investigating the vicinity of the quantum critical point [6,10], but it is crucial to recognize that other regions of the phase diagram may reveal unforeseen and fascinating physical phenomena [2,3].

Recently, Song *et al.* reported that T_o for Nd metal begins to steeply increase above 30 GPa and passes through a maximum (∼180 K) near 70 GPa, before falling towards 0 K near 150 GPa [2], showing a whole Doniach phase diagram. In the same pressure range ($P > 30$ GPa), dilute Nd ions alloyed in superconducting yttrium (Y) induce a remarkable Kondo-like pair-breaking phenomenon. This observation implies that the unusual rise in the magnetic ordering temperature T_o in Nd metal may share a common origin. Specifically, it is attributed to the activation of Kondo correlations as Nd approaches a magnetic instability, resulting in a negative exchange coupling J [2].

As one of heavy lanthanides, trivalent Er adopts hcp structure with a $4f^{11}$ electron configuration at ambient pressure. The magnetic transitions and complex magnetic structures, arising from the localized $4f$ orbital, have been the focus of numerous investigations. A variety of techniques, including elastic neutron scattering [11–15], synchrotron x-ray scattering [16], electrical resistivity [17,18], magnetization [18,19], heat capacity [20,21], and magnetostriction [22–24], have confirmed antiferromagnetism (AFM) below 80 K and ferromagnetism (FM) below 20 K in Er. The equation of state and the following structural phase transitions in Er have been determined to pressures as high as 151 GPa at ambient temperature [25]. The structural transitions have been established: hcp to Sm type at 9 GPa, to dhcp at 29 GPa, to hR24 at 58 GPa, and to monoclinic $C2/m$ at 118 GPa. This sequence, shown at the top of Fig. 3, is typical of trivalent lanthanide metals and results from the increased d character in the conduction band under pressure [26].

Previous studies on magnetism of Er have been limited to pressures below 20 GPa. Neutron diffraction studies indicated a complete suppression of FM below 2 GPa [27–29]. Electrical resistivity measurements showed that the AFM transition temperature decreases with pressure, with a slope of approximately −3 K/GPa below 10 GPa [30,31]. Magnetic susceptibility measurements confirmed that the AFM transition persists up to at least 20 GPa [32,33]. However, due to the limited resolution of ac magnetic susceptibility experiments, the behavior of the AFM transition above 20 GPa remains unclear [33]. The pressure-induced decline in magnetic

*Contact author: jingsong@iphy.ac.cn
†Contact author: jin@iphy.ac.cn

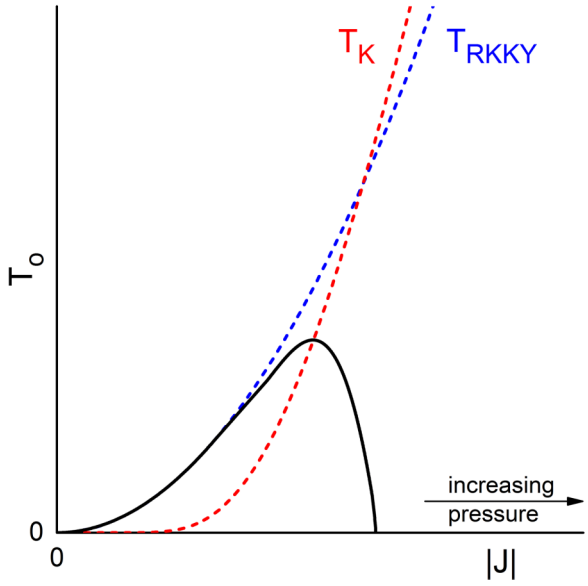

FIG. 1. Magnetic ordering temperature T_o vs absolute value of negative exchange parameter J according to the Kondo lattice model [7]. The competition between RKKY interaction ($T_{RKKY} \propto J^2$) and Kondo effect ($T_K \propto e^{1/JN(E_F)}$) leads to anomalous enhancement and quenching of T_o.

ordering temperature is commonly attributed to a reduction in the electronic density of states at the Fermi level $N(E_F)$ as a result of volume compression [3,33].

In this paper, we present the results of temperature-dependent dc electrical resistivity measurements conducted on Er to pressures as high as 166 GPa. Remarkably, as the applied pressure surpasses approximately 80 GPa, T_o undergoes a significant increase. These findings, along with the giant pair breaking effect in the dilute magnetic alloys Y(0.5 at.% Er), suggest that Er enters into an unconventional magnetic state with an anomalously high magnetic ordering temperature under extreme pressure, distinct from conventional de Gennes scaling.

II. EXPERIMENTAL METHODS

Er samples for the high-pressure resistivity measurements were cut from a polycrystalline Er ingot. The dilute magnetic alloys of Y(Er) were made by argon arc-melting small amounts of Er with Y in argon (both Er and Y 99.9% pure, polycrystalline, Alfa Aesar). Following the initial melt, the sample was turned over and remelted several times to enhance homogeneity. The Er concentration in the bulk sample, as measured by inductively coupled plasma-atomic emission spectrometry (ICP-AES), was determined to be 0.508 at.% with an uncertainty of 0.004 at.%.

To generate pressures well beyond a megabar pressure, a diamond anvil cell (DAC) made of CuBe alloy was used. Five separate high-pressure experiments on Er or Y(Er) were carried out. In runs 1 and 2 pressure was generated by two opposing diamond anvils with 0.30 mm diameter culets. The stainless steel (T301) gasket (250 μm thick) was preindented to 50 μm and a 200 μm diameter hole drilled through the center of the preindentation area. CBN-epoxy mixture was used as insulation material. A hole of 100 μm diameter was drilled and NaCl was filled as a pressure medium. Four gold strips were then placed on the insulation layer, acting as the electrical leads for the four-point resistivity measurement. The Er sample with dimensions 50 × 50 × 5 μm^3 was then placed on the gold strips. In experimental run 3 on elemental Er and in our measurements of Y(Er) alloy, the anvils had 0.10 mm diameter culets beveled to 0.30 mm diameter. The stainless steel (T301) gasket (250 μm thick) was preindented to 30 μm and a 250 μm diameter hole was laser-drilled through the center of the preindentation area. Al_2O_3-epoxy mixture was used as insulation material. A hole of 50 μm diameter was drilled and NaCl was filled as a pressure medium. The inner Au/Ti electrodes were sputtered on the anvil culet with a thickness of 0.5 μm. The Er or Y(Er) sample with dimensions 15 × 15 × 1 μm^3 was then placed on the deposited gold leads, as shown in the inset of Fig. 3. Further details of the high-pressure resistivity techniques can be found elsewhere [2,34]. Pressure was determined by ruby fluorescence [35] in runs 1 and 2 and diamond Raman shift [36] in run 3 and Y(Er). The values of the pressures given are averaged over the sample to an estimated accuracy of ±5%.

High-pressure x-ray absorption near-edge spectroscopy (XANES) experiments on Er's L_3 edge (8.358 keV) used transmission geometry at beam line BL15U1 of Shanghai Synchrotron Radiation Facility (SSRF). Anvils with 80 μm culet diameter beveled to 300 μm and stainless steel (T301) gaskets were used. A piece of Er sample was flattened to approximately 5 μm in thickness and cut to a size of ∼30 × 30 μm^2. Compressed neon (Ne) gas was used as the pressure medium and ruby spheres were placed next to the sample for pressure calibration. When the ruby fluorescence diminished, the diamond Raman shift was used for pressure calibration. The XANES measurements at ambient temperature show that Er remains firmly trivalent to at least 123 GPa.

III. EXPERIMENTAL RESULTS AND DISCUSSION

The temperature-dependent resistance $R(T)$ of Er was measured in three separate experimental runs. Runs 1, 2, and 3 were successfully conducted up to pressures of 20 GPa, 59 GPa, and 166 GPa, respectively. In Fig. 2, $R(T)$ is illustrated over the temperature range of 3.5–295 K and the pressure range of 0–166 GPa. Note that no indications of superconductivity were observed in any of the measurements. Referring to Fig. 2, the initial decrease in $R(T)$ on cooling from room temperature is moderate, followed by a sharp increase in slope dR/dT marked by an anomaly or knee, signaling a reduction in the spin-disorder scattering R_{sd} as magnetic ordering sets in. Here, the magnetic ordering temperature T_o is defined as the temperature where two straight red tangent lines intersect, as illustrated at 59 GPa in run2 and at 102 GPa in run3 in Fig. 2. At some pressures in run2, such as 0.5, 3.1, 5,1, and 7.5 GPa, the increase of resistance with decreasing temperature near T_o is attributed to critical spin fluctuation [31,37]. Fortunately, the transition remains sharp up to the highest pressure 166 GPa in this study, unlike the broadening observed in other trivalent lanthanides such as Nd, Dy, Gd, Tb, and Sm, which have been studied under similar conditions in previous research [2,3,38,39].

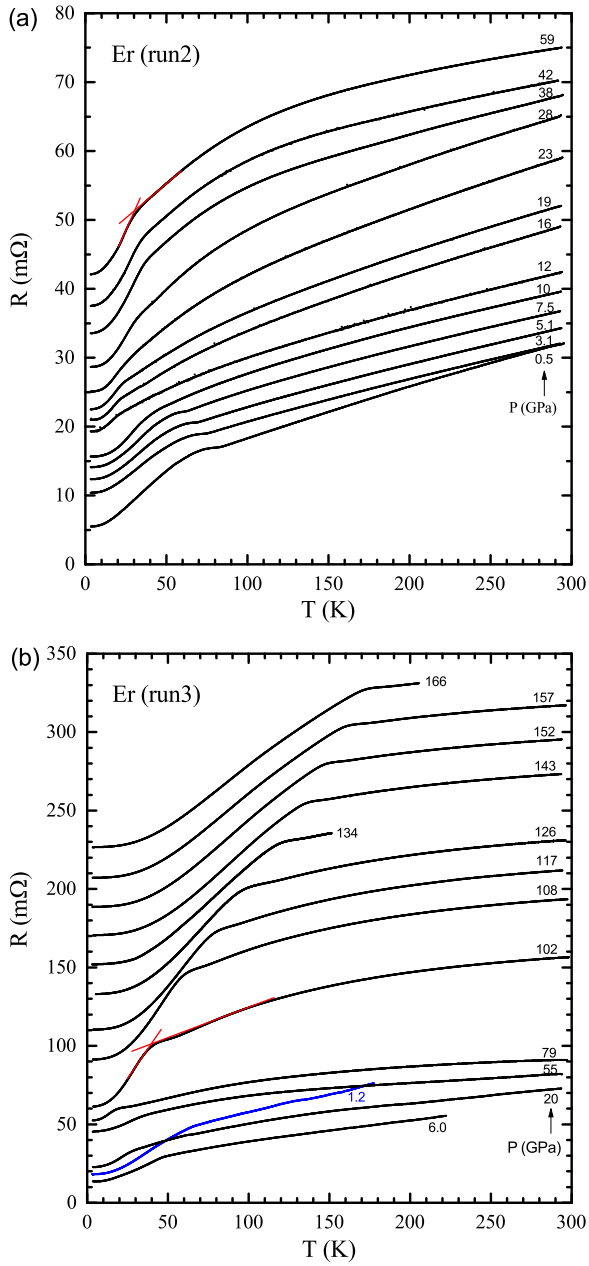

FIG. 2. Resistance of Er from run 2 (a) and run 3 (b) versus temperature to 295 K at various pressures. Data are shifted vertically for clarity; the shift-up values at each pressure are as follows: (a) 0, 6, 8, 10, 11, 13, 13, 14, 13, 13, 11, 11, and 13 mΩ at 0.5, 3.1, 5.1, 7.5, 10, 12, 16, 19, 23, 28, 38, 42, and 59 GPa, respectively; (b) 0, 0, 0, 0, 0, −20, 20, 40, 60, 80, 100, 120, 140, and 160 mΩ at 1.2, 6.0, 20, 55, 79, 102, 108, 117, 126, 134, 143, 152, 157, and 166 GPa, respectively. The magnetic ordering temperature T_o is determined by the intersection point of two straight lines, while the upper and lower error bars for T_o are determined by the tangent points where the straight lines touch the $R(T)$ curve, as illustrated at 59 GPa in panel (a) and at 102 GPa in panel (b).

Referring to Fig. 3, the pressure dependence $T_o(P)$ for Er decreases monotonically below 20 GPa, agreeing reasonably both with earlier magnetic susceptibility measurements of Jackson *et al.* [33] to 20 GPa and with very recent resistivity

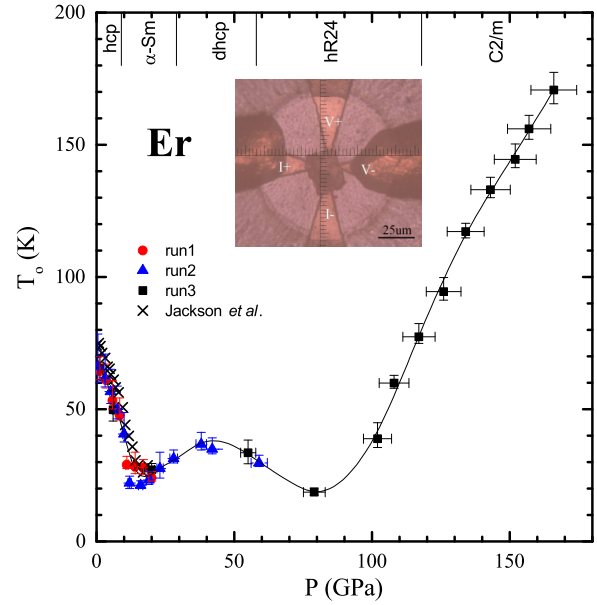

FIG. 3. Magnetic ordering temperature T_o of Er versus pressure. Earlier studies in (x) symbols: Jackson *et al.* [33], and present resistivity measurements in solid symbols: run 1 (red), run 2 (blue), and run 3 (black). The extended solid line through data points is a guide to the eye. The inset shows an image of Er sample resting on four deposited Au leads in run 3 to illustrate the Van de Paw configuration for measuring $R(T)$. Crystal structures at top of graph are for Er [25].

studies of Thomas *et al.* [31] to 10 GPa. The pressure dependence $T_o(P)$ to 80 GPa exhibits a nonmonotonic behavior, passing through a maximum near 40 GPa, gradually decreasing to ∼20 K near 80 GPa. For a conventional lanthanide metal with a stable magnetic moment, the magnetic ordering temperature T_o is expected to scale with the de Gennes factor $(g-1)^2 J_t(J_t+1)$, modulated by the prefactor $J^2 N(E_F)$, where J represents the exchange interaction between the $4f$ ions and conduction electrons, $N(E_F)$ is the density of states at the Fermi energy, g is the Landé g factor, and J_t is the total angular momentum quantum number [33,40]. Since the de Gennes factor remains constant under pressure, unless the magnetic state becomes unstable or a valence transition occurs, the strikingly similar nonmonotonic pressure dependencies of T_o for Er up to 80 GPa, Tb up to 80 GPa [38], Dy up to 70 GPa [3], and Gd up to 60 GPa [3] likely originate from the pressure dependence of the prefactor $J^2 N(E_F)$. This behavior is facilitated by a series of nearly identical structural phase transitions observed in Er [25], Tb [41], Dy [42], and Gd [43] under pressure.

Intriguingly, $T_o(P)$ experiences a sharp upward shift to 171 K at 166 GPa (see again in Fig. 3), suggesting an instability in Er's magnetic state emerges and Er shows anomalous magnetism. In contrast, no such magnetic instabilities are observed in Gd, even under extreme pressures [3], because the local magnetic state of Gd, with its half-filled $4f^7$ orbital, is the most stable among all elements, with the $4f^7$ level lying ∼9 eV below the Fermi level [44]. A similar pronounced upward shift of the anomaly in $R(T)$ was also found in Dy for $P > 70$ GPa [3]. Recent synchrotron Mössbauer spectroscopy (SMS) studies conducted on Dy up to 141 GPa support that

the anomaly in Dy's $R(T)$ at T_o indeed arises from magnetic ordering [45].

In general, the exchange coupling $J = J_+ + J_-$ between a magnetic ion and the conduction electrons includes both the conventional positive exchange interaction J_+ [46] and the negative covalent mixing exchange J_- [47]. For a lanthanide, the negative covalent-mixing exchange component J_- could be determined by $J_- \propto -|V_{sf}|^2/E_{ex}$, where V_{sf} is the mixing matrix element and E_{ex} is the $4f$-electron stabilization energy ($E_{ex} = E_F - E_{4f^{11}}$ for Er^{3+}) [47]. As for the majority of lanthanides at low pressure, the positive exchange dominates, resulting in a positive J, and T_o follows conventional de Gennes scaling [33]. An example of this behavior is seen in the pressure dependence $T_o(P)$ for Er below 80 GPa when compared to other heavy lanthanide metals [33]. However, as the ions magnetic state is pushed toward an instability by applying sufficiently high pressure, E_{ex} approaches zero and/or V_{sf} increases, and thus the covalent-mixing exchange may become dominant, leading to a negative J, whereby the Kondo screening effect strongly competes with the RKKY interactions between ions. Then, the Doniach phase diagram (see Fig. 1) is invoked to illustrate the competition between the RKKY interaction and the Kondo interaction as a function of the total exchange coupling J between magnetic ions and conduction electrons ($J = J_+ + J_- < 0$). Initially, $|J|$ is small, the RKKY interaction dominates, and T_o follows T_{RKKY}. As $|J|$ increases, the Kondo interaction becomes comparable to the RKKY interaction, causing T_o to deviate from T_{RKKY} and reach a maximum. Finally, when the Kondo interaction ($T_K \propto e^{1/JN(E_F)}$) overtakes the RKKY interaction ($T_{RKKY} \propto J^2$), T_o decreases toward zero, marking the complete screening of the local magnetic moment.

In order to test whether in Er the anomalous enhancement of T_o with pressure might signal an approaching instability in the magnetic state of each Er ion, a well-established approach [48,49] to probe the magnetic state of a given ion is to alloy it in dilute concentration with a superconductor that shares closely similar conduction electron properties and then determine the extent of suppression of the superconducting transition temperature, ΔT_c. Yttrium (Y), a superconductor under pressure [2,50,51], is the ideal host for Er since the character of a Y's *spd*-electron conduction band closely matches that of Er. Comparing Figs. 3 and 5, it is seen that Y's structural sequence matches that of Er reasonably well. The pressure dependence of superconductivity was studied in dilute magnetic Y(0.5 at.% Er) alloys to 183 GPa, as illustrated in Fig. 4. T_c is determined as the midpoint of the superconducting transition. All results for $T_c(P)$ are presented in Fig. 5. In the lower-pressure region below 80 GPa, $T_c(P)$ for the Y(Er) alloys reasonably tracks that for pure Y. However, a significant deviation becomes apparent at higher pressures. The suppression of superconductivity continues to increase up to the highest measured pressure. This substantial pair breaking provides clear evidence that Kondo physics becomes prominent for pressures above 80 GPa. A similar phenomenon has been observed in Y(Nd) [2], Y(Dy) [3], Y(Tb) [38], and Y(Sm) [39]. In addition, a key indication that Kondo physics with a negative exchange interaction (J) plays a crucial role in these experiments is the emergence of a resistivity minimum in $R(T)$ at the highest pressures, as depicted in Fig. 6. Above

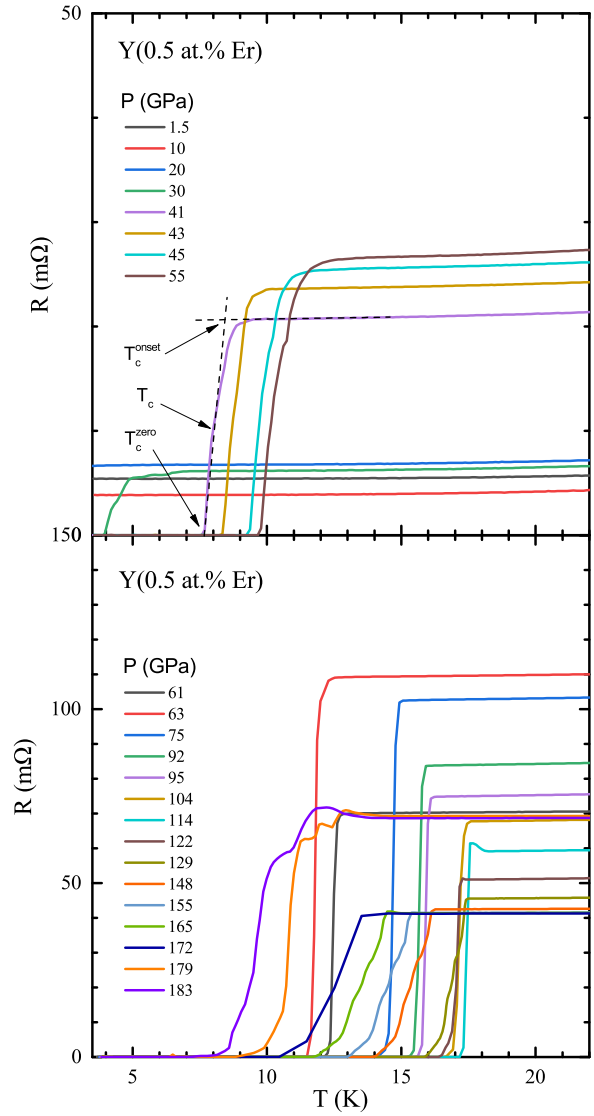

FIG. 4. Four-point resistance versus temperature for Y(0.5 at.% Er) at various pressures. T_c^{onset} is defined as the intersection of two straight dashed lines, T_c^{zero} is defined as the temperature where the sloped dashed line intersects $R = 0$ mΩ, and T_c is determined as the midpoint between T_c^{onset} and T_c^{zero}, as illustrated at 41 GPa. Below T_c^{zero} the resistance vanishes within experimental error.

the superconducting transition temperature of the Y(Er) alloy, the resistance is primarily governed by a significant phonon contribution. Consequently, a precise determination of the Kondo temperature is not feasible due to the overwhelming influence of phonon scattering.

The increase in the magnetic ordering temperature T_o under pressure, predicted by the Doniach model, should theoretically reach a maximum and then decline towards 0 K. Song *et al.* [2] confirmed this experimentally in a light lanthanide Nd showing a whole Doniach phase diagram with similar anomalous behavior in $T_o(P)$. In parallel, the giant pair breaking for Y(Er) alloys seen in Fig. 5 should decrease at even higher pressures. Theoretical work [53,54] has shown that the rise and fall of giant Kondo pair breaking is a result of the passing of the Kondo temperature through the temperature

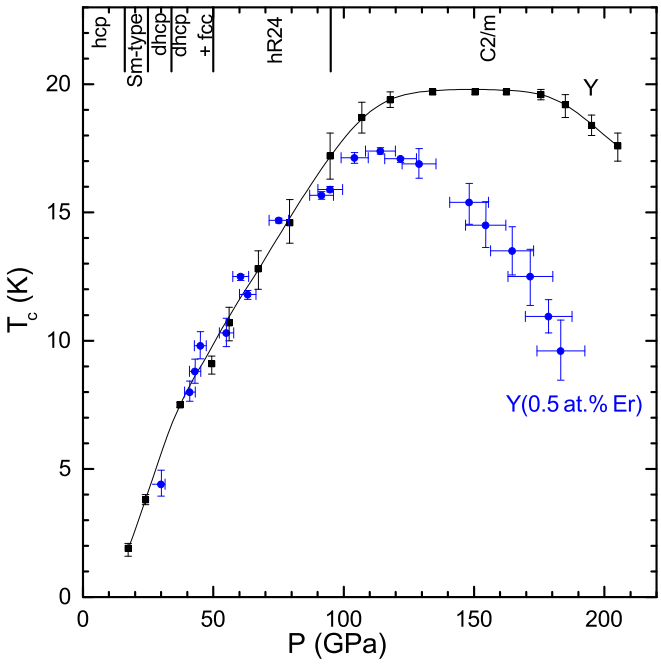

FIG. 5. T_c versus pressure for Y(0.5 at.% Er) compared to that for Y [2]. Above 80 GPa, strong superconducting pair breaking $\Delta T_c = T_c(\mathrm{Y}) - T_c[\mathrm{Y(Er)}]$ occurs. T_c^{onset} and T_c^{zero} defined in Fig. 4 provide the upper and lower error bars of T_c. At the top of the graph are crystal structures taken on by superconducting host Y [52].

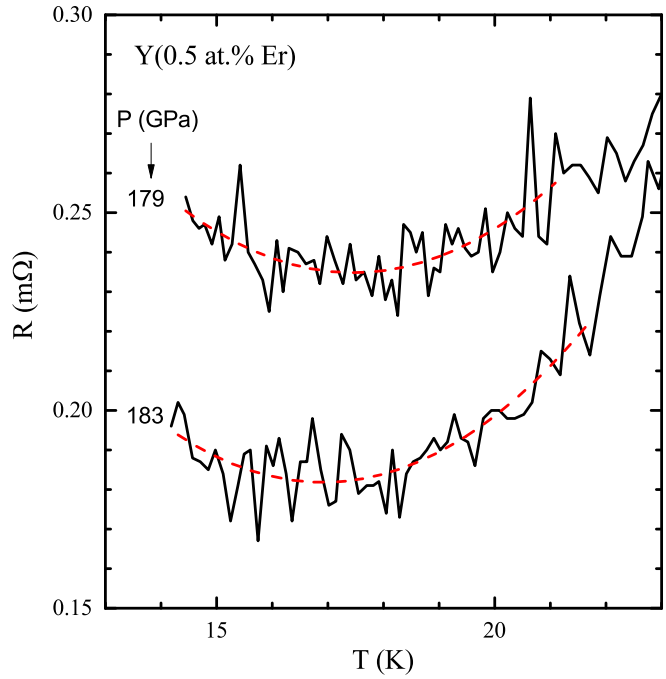

FIG. 6. Resistance of Y (0.5 at.% Er) as a function of temperature at 179 GPa and 183 GPa exhibits characteristic Kondo minima. Data are shifted vertically for clarity; the shift-down values are 69.04 mΩ for 179 GPa and 68.50 mΩ for 183 GPa, respectively. The red dashed curves serve as a visual guide to highlight the Kondo minima.

region near T_c. This rise and fall of ΔT_c has been clearly demonstrated in experimental results on La(Ce) [55], Y(Dy) [3], and Y(Nd) [2] alloys, etc. The extent of pair breaking ΔT_c per atomic percent here is very large, reaching to a maximum value of ∼19 K/(at.% magnetic impurity) at about 183 GPa.

The anomalous enhancement of T_o in Er and the onset of robust superconducting pair breaking in Y(Er) alloys both commence at approximately the same pressure range of 80 GPa. This alignment implies a common mechanism: at this pressure, the exchange parameter (J) has likely turned negative, triggering intense Kondo correlations that substantially alter the exchange interactions among Er ions. We propose that, as the magnitude of $|J|$ increases with pressure, T_o initiates a steep ascent along the left side of the Doniach phase diagram depicted in Fig. 1. In this framework, the same negative exchange parameter J is accountable for both the markedly enhanced magnetic ordering and the occurrence of giant pair breaking when $|J|$ attains a sufficiently large value.

To rule out the possibility of a valence transition ($4f^{11} \rightarrow 4f^{10}$) that could lead to a remarkable increase in the ordering temperature based on de Gennes scaling [33,40], we conducted XANES studies at pressures up to 123 GPa. As shown in Fig. 7, no additional absorption peak (4+) was observed up to 123 GPa, indicating that Er remains trivalent at these pressures. In contrast, valence transitions have been reported in Yb [5] and Eu [57,58], where clear XANES features associated with valence changes were identified. The L_3 absorption edge is dominated by the dipolar $2p_{3/2} \rightarrow 5d$ electronic excitation; thus the feature of the absorption peak is directly related to the characteristics of the $5d$ band. The absorption peak center shifts toward higher energy slightly, indicating an increase in the $5d$ band bottom energy [26].

The reduction in the white line peak intensity is attributed to $s-d$ electron transfer [26,56], resulting in increased $5d$ state occupancy and reduced L_3 edge absorption. The broadening of the absorption peak with increasing pressure is primarily attributed to the broadening of the $5d$ band bottom [26],

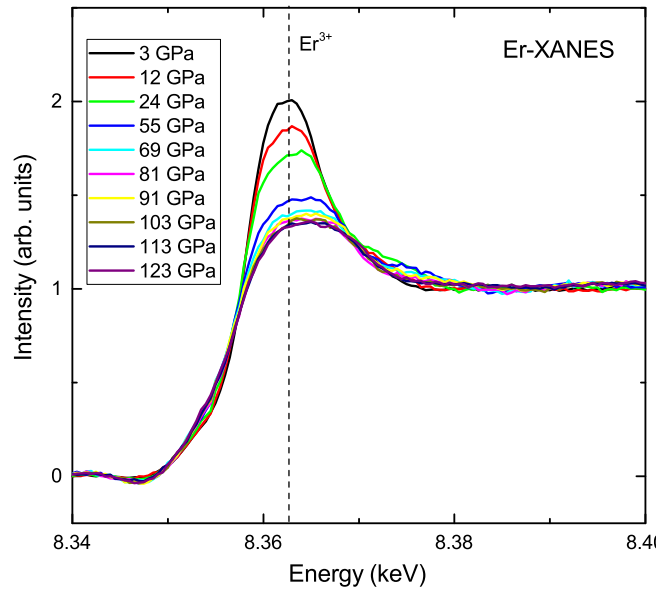

FIG. 7. Pressure dependence of L_3 XANES data showing that Er remains trivalent ($4f^{11}$) to at least 123 GPa. No 4+ or mixed valence state is observed. Pressure-induced reduction of peak height is a direct measure of $s \rightarrow d$ transfer [26,56].

while pressure-induced inhomogeneities or disorder may also contribute to some extent.

Could perhaps an alternative explanation, such as the crystal electric field splitting effect or the Anderson localization due to local disorders, account for the anomalously high magnetic ordering temperatures T_o in Er? First, in the crystal electric field scenario, a maximum enhancement of T_o would be expected to be approximately $3J_t/(J_t+1) = 2.6$ [3,59] for trivalent Er ($S = 3/2$, $L = 6$, and thus $J_t = 15/2$). However, the observed enhancement of T_o above 80 GPa is approximately $T_o(166\ \text{GPa})/T_o(80\ \text{GPa}) \approx 8$, which is significantly higher. Moreover, in this crystal electric field scenario, it is difficult to understand a negligible pair breaking below 80 GPa and a strong increase of the pair breaking above 80 GPa in the dilute magnetic alloy Y (0.5 at.% Er). Second, in the case of the Anderson localization due to local disorders, it would apply to Gd as well, which should lead to an anomalous rise in T_o for Gd under extreme pressure. However, no such rise in T_o has been observed in Gd [3,56]. Therefore, we propose that the observed behavior in Er is more consistent with a Kondo physics scenario.

IV. CONCLUSION

In summary, the magnetic ordering temperature (T_o) of Er exhibits a notable increase starting at around 80 GPa. The involvement of Kondo physics is supported by the resemblance to the Doniach phase diagram and the giant superconducting pair breaking observed in dilute Y(Er) alloys under extreme pressures. This study contributes to the understanding of the Kondo lattice behavior and unveils an unrecognized feature, an anomalous enhancement of magnetic ordering, providing another perspective for designing magnetic materials with high ordering temperature.

ACKNOWLEDGMENTS

The authors would like to thank L. Song and Y.-C. Lau for preparing the Y(Er) alloy. This work was supported by the National Natural Science Foundation of China (Grant No. 12204514) and the National Key Research and Development Program of China (Grant No. 2023YFA1406000). The authors thank the staff at BL15U1 and the User Experiment Assist System of Shanghai Synchrotron Radiation Facility (SSRF).

[1] P. Aynajian, E. da Silva Neto, A. Gyenis, R. E. Baumbach, J. D. Thompson, Z. Fisk, E. D. Bauer, and A. Yazdani, Visualizing heavy fermions emerging in a quantum critical Kondo lattice, Nature (London) **486**, 201 (2012).

[2] J. Song, W. Bi, D. Haskel, and J. S. Schilling, Evidence for strong enhancement of the magnetic ordering temperature of trivalent Nd metal under extreme pressure, Phys. Rev. B **95**, 205138 (2017).

[3] J. Lim, G. Fabbris, D. Haskel, and J. S. Schilling, Magnetic ordering at anomalously high temperatures in Dy at extreme pressures, Phys. Rev. B **91**, 045116 (2015).

[4] D. J. Scalapino, A common thread: The pairing interaction for unconventional superconductors, Rev. Mod. Phys. **84**, 1383 (2012).

[5] J. Song, G. Fabbris, W. Bi, D. Haskel, and J. S. Schilling, Pressure-induced superconductivity in elemental ytterbium metal, Phys. Rev. Lett. **121**, 037004 (2018).

[6] S. Sachdev and B. Keimer, Quantum criticality, Phys. Today **64**(2), 29 (2011).

[7] S. Doniach, The Kondo lattice and weak antiferromagnetism, Physica B+C **91**, 231 (1977).

[8] J. R. Iglesias, C. Lacroix, and B. Coqblin, Revisited Doniach diagram: Influence of short-range antiferromagnetic correlations in the Kondo lattice, Phys. Rev. B **56**, 11820 (1997).

[9] Y. Yang, Z. Fisk, H. Lee, J. Thompson, and D. Pines, Scaling the Kondo lattice, Nature (London) **454**, 611 (2008).

[10] S. Sachdev, *Quantum Phase Transitions*, 2nd ed. (Cambridge University Press, Cambridge, 2011).

[11] J. W. Cable, E. O. Wollan, W. C. Koehler, and M. K. Wilkinson, Magnetic structures of metallic erbium, Phys. Rev. **140**, A1896 (1965).

[12] M. Habenschuss, C. Stassis, S. K. Sinha, H. W. Deckman, and F. H. Spedding, Neutron diffraction study of the magnetic structure of erbium, Phys. Rev. B **10**, 1020 (1974).

[13] H. Lin, M. F. Collins, T. M. Holden, and W. Wei, Magnetic structure of erbium, Phys. Rev. B **45**, 12873 (1992).

[14] R. A. Cowley and J. Jensen, Magnetic structures and interactions in erbium, J. Phys.: Condens. Matter **4**, 9673 (1992).

[15] J. Jensen and R. A. Cowley, Non-planar magnetic structures and trigonal interactions in erbium, Europhys. Lett. **21**, 705 (1993).

[16] D. Gibbs, J. Bohr, J. D. Axe, D. E. Moncton, and K. L. D'Amico, Magnetic structure of erbium, Phys. Rev. B **34**, 8182 (1986).

[17] R. V. Colvin, S. Legvold, and F. H. Spedding, Electrical resistivity of the heavy rare-earth metals, Phys. Rev. **120**, 741 (1960).

[18] R. W. Green, S. Legvold, and F. H. Spedding, Magnetization and electrical resistivity of erbium single crystals, Phys. Rev. **122**, 827 (1961).

[19] B. Watson and N. Ali, Magnetic transitions in single-crystal erbium, J. Phys.: Condens. Matter **7**, 4713 (1995).

[20] R. E. Skochdopole, M. Griffel, and F. H. Spedding, Heat capacity of erbium from 15 to 320°K, J. Chem. Phys. **23**, 2258 (1955).

[21] H. U. Astrom and G. Benediktsson, On magnetic first-order transitions in erbium, J. Phys.: Condens. Matter **1**, 4381 (1989).

[22] J. J. Rhyne and S. Legvold, Magnetostriction of erbium single crystals, Phys. Rev. **140**, A2143 (1965).

[23] R. S. Eccleston and S. B. Palmer, Magnetoelastic effects in single-crystal erbium, J. Phys.: Condens. Matter **4**, 10037 (1992).

[24] S. Zochowski and K. McEwen, Dilatometric study of the magnetic phase diagram of erbium, J. Magn. Magn. Mater. **140–144**, 1127 (1995), International Conference on Magnetism.

[25] G. K. Samudrala, S. A. Thomas, J. M. Montgomery, and Y. K. Vohra, High pressure phase transitions in the rare earth metal erbium to 151 GPa, J. Phys.: Condens. Matter **23**, 315701 (2011).

[26] J. C. Duthie and D. G. Pettifor, Correlation between d-band Occupancy and crystal structure in the rare earths, Phys. Rev. Lett. **38**, 564 (1977).
[27] S. Kawano, B. Lebech, and N. Achiwa, Magnetic structures of erbium under high pressure, J. Phys.: Condens. Matter **5**, 1535 (1993).
[28] S. Kawano, S. Sørensen, B. Lebech, and N. Achiwa, High pressure neutron diffraction studies of the magnetic structures of erbium, J. Magn. Magn. Mater. **140–144**, 763 (1995), International Conference on Magnetism.
[29] M. Ellerby, K. A. Mcewen, J. Jensen, and M. J. Bull, Neutron diffraction study of the p - T phase diagram for erbium, High Press. Res. **22**, 369 (2002).
[30] M. Ellerby, K. A. McEwen, E. Bauer, R. Hauser, and J. Jensen, Pressure-dependent resistivity and magnetoresistivity of erbium, Phys. Rev. B **61**, 6790 (2000).
[31] S. A. Thomas, G. M. Tsoi, L. E. Wenger, Y. K. Vohra, and S. T. Weir, Magnetic and structural phase transitions in erbium at low temperatures and high pressures, Phys. Rev. B **84**, 144415 (2011).
[32] J. E. Milton and T. A. Scott, Pressure dependence of the magnetic transitions in dysprosium and erbium, Phys. Rev. **160**, 387 (1967).
[33] D. D. Jackson, V. Malba, S. T. Weir, P. A. Baker, and Y. K. Vohra, High-pressure magnetic susceptibility experiments on the heavy lanthanides Gd, Tb, Dy, Ho, Er, and Tm, Phys. Rev. B **71**, 184416 (2005).
[34] X. He, C. L. Zhang, Z. W. Li, S. J. Zhang, B. S. Min, J. Zhang, K. Lu, J. F. Zhao, L. C. Shi, Y. Peng, X. C. Wang, S. M. Feng, J. Song, L. H. Wang, V. B. Prakapenka, S. Chariton, H. Z. Liu, and C. Q. Jin, Superconductivity observed in tantalum polyhydride at high pressure, Chin. Phys. Lett. **40**, 057404 (2023).
[35] G. Shen, Y. Wang, A. Dewaele, C. Wu, D. E. Fratanduono, J. Eggert, S. Klotz, K. F. Dziubek, P. Loubeyre, O. V. Fat'yanov, P. D. Asimow, T. Mashimo, R. M. M. Wentzcovitch, and other members of the IPPS task group, Toward an international practical pressure scale: A proposal for an IPPS ruby gauge, High Press. Res. **40**, 299 (2020).
[36] Y. Akahama and H. Kawamura, Pressure calibration of diamond anvil Raman gauge to 310 GPa, J. Appl. Phys. **100**, 043516 (2006).
[37] O. Rapp, G. Benediktsson, H. U. Åström, S. Arajs, and K. V. Rao, Electrical resistivity of antiferromagnetic chromium near the Néel temperature, Phys. Rev. B **18**, 3665 (1978).
[38] J. Lim, G. Fabbris, D. Haskel, and J. S. Schilling, Anomalous pressure dependence of magnetic ordering temperature in Tb revealed by resistivity measurements to 141 GPa: Comparison with Gd and Dy, Phys. Rev. B **91**, 174428 (2015).
[39] Y. Deng and J. S. Schilling, Enhanced magnetic ordering in Sm metal under extreme pressure, Phys. Rev. B **99**, 085137 (2019).
[40] K. N. Taylor and M. I. Darby, *Physics of Rare Earth Solids* (Chapman and Hall Ltd, London, 1972).
[41] N. C. Cunningham, W. Qiu, K. M. Hope, H.-P. Liermann, and Y. K. Vohra, Symmetry lowering under high pressure: Structural evidence for f-shell delocalization in heavy rare earth metal terbium, Phys. Rev. B **76**, 212101 (2007).
[42] R. Patterson, C. K. Saw, and J. Akella, Static high-pressure structural studies on Dy to 119 GPa, J. Appl. Phys. **95**, 5443 (2004).
[43] D. Errandonea, R. Boehler, B. Schwager, and M. Mezouar, Structural studies of gadolinium at high pressure and temperature, Phys. Rev. B **75**, 014103 (2007).
[44] Z. P. Yin and W. E. Pickett, Stability of the Gd magnetic moment to the 500 GPa regime: An LDA + U correlated band method study, Phys. Rev. B **74**, 205106 (2006).
[45] W. Bi *et al.* (unpublished).
[46] A. J. Freeman and R. B. Frankel, in *Hyperfine Interactions* (Academic Press, New York, 1967).
[47] J. R. Schrieffer and P. A. Wolff, Relation between the Anderson and Kondo Hamiltonians, Phys. Rev. **149**, 491 (1966).
[48] M. B. Maple, Superconductivity: A probe of the magnetic state of local moments in metals, Appl. Phys. **9**, 179 (1976).
[49] B. T. Matthias, H. Suhl, and E. Corenzwit, Spin exchange in superconductors, Phys. Rev. Lett. **1**, 92 (1958).
[50] J. Wittig, Pressure-induced superconductivity in cesium and yttrium, Phys. Rev. Lett. **24**, 812 (1970).
[51] J. Hamlin, V. Tissen, and J. Schilling, Superconductivity at 20 K in yttrium metal at pressures exceeding 1Mbar, Physica C **451**, 82 (2007).
[52] G. K. Samudrala, G. M. Tsoi, and Y. K. Vohra, Structural phase transitions in yttrium under ultrahigh pressures, J. Phys.: Condens. Matter **24**, 362201 (2012).
[53] M. J. Zuckermann, Magnetic impurities and superconductivity below the Kondo temperature. Nagaoka's model, Phys. Rev. **168**, 390 (1968).
[54] E. Müller-Hartmann and J. Zittartz, Theory of magnetic impurities in superconductors. II, Z. Physik **234**, 58 (1970).
[55] M. B. Maple, J. Wittig, and K. S. Kim, Pressure-induced magnetic-nonmagnetic transition of Ce impurities in La, Phys. Rev. Lett. **23**, 1375 (1969).
[56] G. Fabbris, T. Matsuoka, J. Lim, J. R. L. Mardegan, K. Shimizu, D. Haskel, and J. S. Schilling, Different routes to pressure-induced volume collapse transitions in gadolinium and terbium metals, Phys. Rev. B **88**, 245103 (2013).
[57] W. Bi, N. M. Souza-Neto, D. Haskel, G. Fabbris, E. E. Alp, J. Zhao, R. G. Hennig, M. M. Abd-Elmeguid, Y. Meng, R. W. McCallum, K. Dennis, and J. S. Schilling, Synchrotron x-ray spectroscopy studies of valence and magnetic state in europium metal to extreme pressures, Phys. Rev. B **85**, 205134 (2012).
[58] B. Chen, M. Tian, J. Zhang, B. Li, Y. Xiao, P. Chow, C. Kenney-Benson, H. Deng, J. Zhang, R. Sereika, X. Yin, D. Wang, X. Hong, C. Jin, Y. Bi, Hanyu Liu, Haifeng Liu, J. Li, K. Jin, Q. Wu *et al.*, Novel valence transition in elemental metal europium around 80 GPa, Phys. Rev. Lett. **129**, 016401 (2022).
[59] B. D. Dunlap, L. N. Hall, F. Behroozi, G. W. Crabtree, and D. G. Niarchos, Crystal-field effects and the magnetic properties of rare-earth rhodium borides, Phys. Rev. B **29**, 6244 (1984).